

Optimization and design of solar water heating system for Dar Ghadames Hotel

Edris M. S. Ali ¹, G. E. A. Muftah ^{*2}

¹ Energy Management Department, Faculty of Engineering, University of Tripoli, Tripoli Libya

² Physics Department, Faculty of Science, University of Bani Waleed, Bani Waleed, Libya

*Corresponding author: muftah-geam4676@hotmail.com

تصميم نظام تسخين المياه بالطاقة الشمسية لفندق دار غدامس-ليبيا

إدريس محمد صالح علي ¹، جعفر الصيد عوض مفتاح ^{*2}

¹ قسم إدارة الطاقة، كلية الهندسة، جامعة طرابلس، طرابلس، ليبيا

² قسم الفيزياء، كلية العلوم، جامعة بني وليد، بني وليد، ليبيا

Received: 22-12-2025; Accepted: 03-03-2026; Published: 17-03-2026

Abstract

In this study, the solar water heating system for Dar Ghadames Hotel was optimized using the f-chart method to convert solar energy into hot water to meet the hotel's demand. The optimal collector area was determined under the local climatic conditions of Ghadames. A flat plate collector was selected for this project after comparing the advantages and disadvantages of other types of collectors.

Solar radiation data was collected through the National Meteorological Centre in Tripoli and utilized to calculate the monthly average solar radiation outside the atmosphere and the monthly average solar radiation inside the atmosphere on a horizontal surface. The study analyzed the monthly average solar radiation inside the atmosphere at different tilted surface angles and selected the optimal tilt angle to achieve the suitable annual solar energy rate. Based on this, the hotel's hot water consumption rate was estimated, and the amount of solar energy required to meet the hotel's load was calculated. Then, using the f-chart method, the optimal collector area was determined to cover the maximum possible load throughout the year.

Keywords: solar water heating system, solar radiation, optimal collector area, Dar Ghadames Hotel, f-chart method.

المخلص

تم في هذه الدراسة تحسين نظام تسخين المياه بالطاقة الشمسية لفندق دار غدامس باستخدام طريقة الرسم البياني f لتحويل الطاقة الشمسية إلى مياه ساخنة لتغطية الطلب بفندق دار غدامس. وقد تم الحصول على مساحة المجمع المثلى في ظل ظروف المناخ المحلي في غدامس. وقد تم اختيار المجمع الشمسي ذي اللوحة المسطحة (FPC) لهذا المشروع بعد مقارنة المميزات والعيوب بالنسبة للمجمعات الأخرى.

تم جمع بيانات الإشعاع الشمسي عن طريق المركز الوطني للأرصاد الجوية بطرابلس واستخدامها حيث تم حساب المتوسط الشهري للإشعاع الشمسي خارج الغلاف الجوي ومتوسط الإشعاع الشمسي الشهري داخل الغلاف الجوي على سطح أفقي بحيث تتم دراسة المتوسط الشهري للإشعاع الشمسي داخل الغلاف الجوي على زوايا سطح مائلة مختلفة واختيار زاوية الميل المثلى والتي من خلالها يمكن الحصول على المعدل السنوي المناسب من الطاقة الشمسية وبناء عليه تم تقدير معدل استهلاك الماء الساخن بالفندق وحساب كمية الطاقة الشمسية اللازمة لتغطية الحمل بالفندق ثم بعد ذلك وباستخدام طريقة الرسم البياني f-تم تحديد المساحة المثلى للمجمع والتي من خلالها يمكن تغطية أقصى حد ممكن من الحمل على طول العام.

الكلمات المفتاحية: نظام تسخين المياه بالطاقة الشمسية، الإشعاع الشمسي، مساحة المجمع الأمثل، فندق دار غدامس، طريقة مخطط f.

Introduction

Our country, Libya, enjoys immense potential that enables it to develop renewable energy sources. It receives a plentiful amount of direct sunlight, which in turn generates a substantial amount of solar energy. North Africa has the continent's greatest potential for developing solar and wind energy [1]. The average annual solar radiation in the region is about 2,200 kilowatt-hours per square meter. The average wind speed is 7 meters per second, and reaches 9.5 meters per second in Algeria and Libya [2].

Considering that Libya is one of the oil-producing and exporting countries and relies on it as a primary source of income, and due to the fluctuations in oil prices, its finite nature, and its impact on the global environment in terms of global warming and climate change, as well as the global trend towards finding clean alternatives to energy, the thought of finding alternative energy sources has begun. These alternatives aim to replace traditional energy sources, reduce their negative impacts, and achieve sustainable development for communities.

Libya needs to implement significant changes and take important measures to reposition itself regarding energy usage and diversifying its sources of income. This includes providing incentives for investment in renewable energy to make it competitive and redirecting subsidies from electricity generated by oil and gas to renewable energy. These measures are essential to building investor confidence and attracting their participation in renewable energy projects. Investing in these potentials significantly reduces dependence on fossil fuels, contributing to a cleaner environment and paving the way for new action plans for social and economic growth.

This study aims to contribute to encouraging the state to move forward and take important steps towards adopting solar energy as one of the most important types of renewable energy sources, making it a major source of energy in Libya. Dar Ghadames Hotel was chosen to conduct the study due to its location in the city of Ghadames.

Research method

This study aims to calculate the energy that can be extracted from the incident solar radiation (solar radiation) under the local climate conditions of Ghadames city and convert it into thermal energy. For this purpose, the characteristics of the local climate and the solar panel were analysed. Solar collectors consist of several components, as we will see in the third chapter, to deal with solar radiation and convert it into thermal energy. The conversion efficiency varies from one collector to another, as well as from one place to another and other factors that will be studied in this project. Figure 1 shows the model that was chosen for this study.

The first stage is determining the attractive location for investment

It is a study in which the initial opinion was collected, and the suitability of the site for the project was stated in terms of area, availability of data, and review of the information available locally through the National Centre for Meteorology in Tripoli.

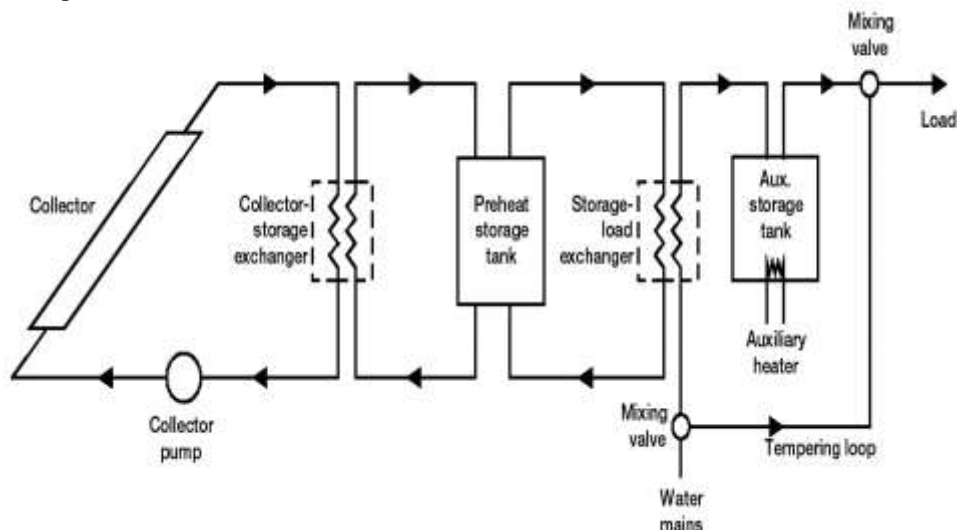


Figure 1 standard configuration of domestic hot water system.

The second stage is calculations and estimates.

- Estimating the amount of solar energy available on the horizontal level of the selected site.
- Estimating the amount of solar energy available on the inclined surface.
- Choosing the optimal angle of inclination for the system.

Third stage the f-chart method which includes:

- Excel data sheet.
- Studying the load and choosing the appropriate area for the system.
- Matching the appropriate collector for the site.

Theoretical aspect

In order to define the declination angle, the correlation 1 was used. The declination is the angular position of the sun at solar noon with respect to the plane of the equator as shown in figure 2. Actually the declination angle gives an idea about time of year. it respects seasonal affect on insolation energy. It ranges from a maximum of 23.45 degrees on July 21 to a minimum of -23.45 degrees on December 21.

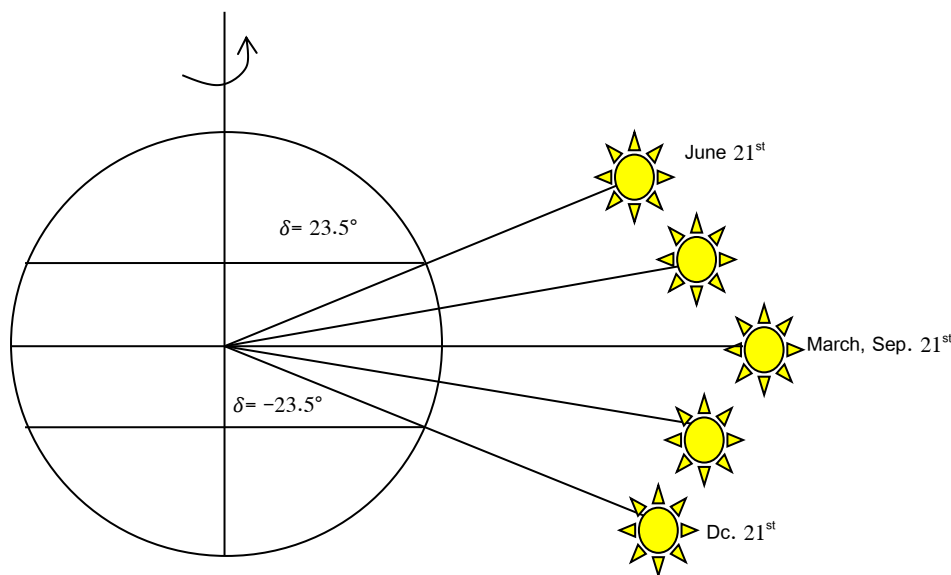


Figure 2 The solar Declination angle.

The solar declination can be calculated by cooper's Equation (1969) [3]:

$$\delta = 23.45 \sin \left(360 \times \frac{(284+n)}{365} \right) \quad (1)$$

Where (n) is the day of year.

The lines of latitude are imaginary lines parallel to the equator and are used to determine locations on the Earth's surface. Latitude ranges from 0 degrees at the equator to 90 degrees north or south at the North and South Poles φ .

Sun angle at sunset

$$\omega_s = \cos^{-1}(-\tan\varphi \tan\delta) \quad (2)$$

Where (φ) is the latitude and δ is the declination.

After obtaining the sunset angle, the number of daylight hours can be determined using the following equation:

$$N_s = \frac{2\omega_s}{15} \quad (3)$$

Extraterrestrial radiation is the theoretical amount of solar energy that would be available on a horizontal plane on the earth's surface if the earth were not surrounded by an atmosphere. In reality, solar radiation undergoes attenuation as it propagates through the atmosphere, resulting in a decrease of its intensity when measured on a plane on the earth's surface. At any specific time within the day, extraterrestrial irradiance can be given by [4];

$$\bar{H}_o = \frac{24 \times 3600}{\pi} G_{sc} \left(1 + 0.033 \cos \left(\frac{360 \times n}{365} \right) \right) \left(\cos\varphi \cos\delta \sin\omega_s + \frac{\pi}{180} \omega_s \sin\varphi \sin\delta \right) \quad (4)$$

Where $G_{sc} = 1367 \text{ w/m}^2$, φ = latitude

Clearness index for each month is influenced by atmosphere characteristics and has a high value under clear weather conditions and a low value under cloudy conditions, with its value ranging from 0.3 to 0.8. It is defined as the ratio of the average daily or monthly radiation to the average daily or monthly extraterrestrial radiation \bar{K}_T .

Monthly average clearness index \bar{K}_T .

$$\bar{K}_T = \frac{\bar{H}}{\bar{H}_o} \quad (5)$$

Where \bar{H} and \bar{H}_o represents monthly average values over an horizontal surface.

According to latitude ($\varphi = 30^\circ$), the \bar{K}_T can be obtained from table 1.

Table 1 Clearance index for different latitude.

| Clear index KT | | | | | | | | | | | | |
|----------------|------|------|------|------|------|------|------|------|------|------|------|------|
| Latitude | Jan | Feb | Mar | Apr | May | Jun | Jul | Aug | Sep | Oct | Nov | Dec |
| S8.8 | 0.52 | 0.53 | 0.52 | 0.53 | 0.55 | 0.49 | 0.42 | 0.38 | 0.43 | 0.47 | 0.52 | 0.5 |
| N30.0 | 0.56 | 0.6 | 0.61 | 0.63 | 0.66 | 0.68 | 0.67 | 0.66 | 0.66 | 0.65 | 0.59 | 0.56 |
| N9.0 | 0.59 | 0.6 | 0.57 | 0.54 | 0.52 | 0.45 | 0.37 | 0.38 | 0.46 | 0.61 | 0.68 | 0.64 |
| S1.3 | 0.63 | 0.62 | 0.59 | 0.52 | 0.49 | 0.46 | 0.39 | 0.4 | 0.51 | 0.54 | 0.52 | 0.61 |
| N33.6 | 0.51 | 0.54 | 0.56 | 0.58 | 0.58 | 0.59 | 0.61 | 0.61 | 0.61 | 0.56 | 0.54 | 0.48 |
| N6.1 | 0.46 | 0.47 | 0.46 | 0.46 | 0.47 | 0.43 | 0.36 | 0.34 | 0.37 | 0.44 | 0.51 | 0.48 |
| N14.7 | 0.62 | 0.67 | 0.68 | 0.67 | 0.65 | 0.6 | 0.53 | 0.5 | 0.52 | 0.6 | 0.6 | 0.59 |
| S25.8 | 0.55 | 0.56 | 0.57 | 0.57 | 0.65 | 0.67 | 0.69 | 0.67 | 0.63 | 0.57 | 0.57 | 0.57 |
| N13.6 | 0.68 | 0.7 | 0.7 | 0.68 | 0.67 | 0.64 | 0.61 | 0.61 | 0.64 | 0.67 | 0.7 | 0.7 |
| N6.9 | 0.51 | 0.51 | 0.55 | 0.55 | 0.6 | 0.63 | 0.66 | 0.64 | 0.61 | 0.59 | 0.58 | 0.53 |
| N0.1 | 0.5 | 0.48 | 0.48 | 0.47 | 0.47 | 0.48 | 0.46 | 0.46 | 0.48 | 0.48 | 0.48 | 0.49 |

The amount of solar radiation falling on a horizontal surface changes annually based on location and seasons, due to its proximity to or distance from the equator. The solar path varies with the seasons, influenced by the summer and winter solstices, and the length of day and night throughout the year. At the equator, the solar angle on a horizontal surface is 90 degrees throughout the year, whereas it is less than 90 degrees on a horizontal surface at the Tropic of Cancer and Tropic of Capricorn. The hemisphere that is tilted toward the Sun receives more solar radiation than the hemisphere that is tilted away from the Sun. Thus, the amount of solar energy received on a horizontal surface is greater in summer than in winter because the hemisphere tilted towards the sun receives more solar energy, while the opposite hemisphere, tilted away from the sun, receives less solar radiation in winter.

The tilt angle of a surface significantly affects the amount of incident solar radiation. The maximum annual solar energy is obtained when the tilt angle equals the latitude of the location, assuming fixed, non-adjustable tilt angles. By selecting the optimal tilt angle, the goal is to have the incoming solar radiation perpendicular to the surface. However, due to Earth's movement, this angle constantly changes, affecting the annual energy output. It is known that the solar radiation incident on a surface is the sum of the direct, diffuse, and reflected components of the total solar radiation, as shown in the figure 3.

By method of Liu and Jordan (1962) as extended by Klein (1977) [5], which has been widely used. If the diffuse and ground-reflected radiation are each assumed to be isotropic, the monthly mean solar radiation on an unshaded tilted surface can be expressed as in the correlation 6 [6].

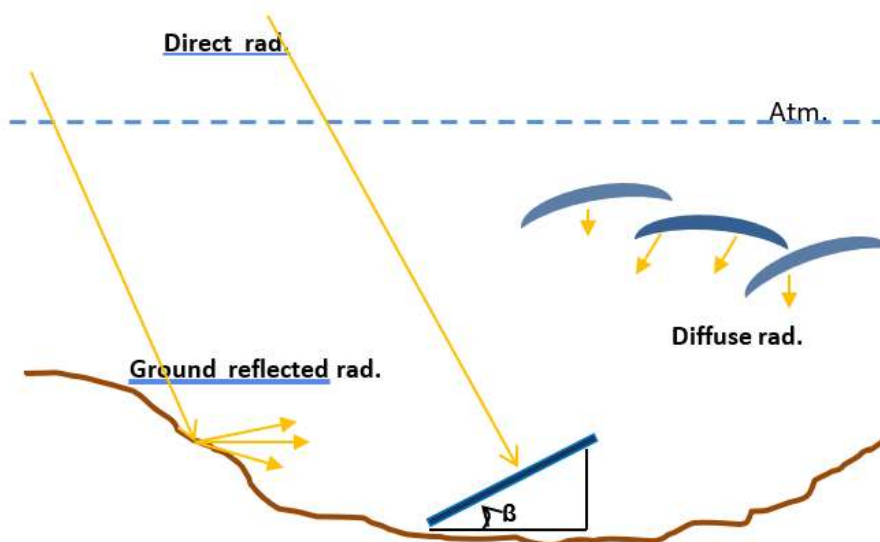


Figure 3 solar radiation on a tilt surface [7].

There are many mathematical models for calculating the total amount of radiation, depending on how terms and periods are handled, each of which relies on different assumptions.

$$\bar{H}_T = \bar{R} \bar{H} \quad (6)$$

\bar{R} the ratio of total radiation on the tilted surface to that on the horizontal surface. Assuming that the emitted radiation and the reflected radiation from the Earth have the same properties, the \bar{R} will be;

$$\bar{R} = \frac{\bar{H}_T}{\bar{H}} = \left(1 - \frac{\bar{H}_d}{\bar{H}}\right) R_b + \frac{\bar{H}_d}{\bar{H}} \left[\frac{1+\cos(\beta)}{2}\right] + \rho_G \left[\frac{1-\cos(\beta)}{2}\right] \quad (7)$$

The correlation 7 represents the components of total radiation, where the first part represents direct radiation, the second part represents diffuse radiation, and the third part represents reflected radiation.

$\frac{\bar{H}_d}{\bar{H}}$ is a function of \bar{K}_T , it is the ratio of daily total diffuse to daily total radiation.

$$\frac{\bar{H}_d}{\bar{H}} = 1.188 - 2.272\bar{K}_T + 9.473\bar{K}_T^2 - 21.865\bar{K}_T^3 + 14.648\bar{K}_T^4 \quad (8)$$

The numerator of correlation 8 is the extraterrestrial radiation on the tilted surface, and the denominator is that on the horizontal surface.

The ratio of the average daily beam radiation on the tilted surface to that on a horizontal surface for the month is R_b ;

$$R_b = \frac{\cos(\varphi-\beta) \cos(\delta) \sin(\omega'_s) + (\pi/180)\omega'_s \sin(\varphi-\beta) \sin(\delta)}{\cos(\varphi) \cos(\delta) \sin(\omega_s) + (\pi/180)\omega_s \sin(\varphi) \sin(\delta)} \quad (9)$$

where (ω'_s) is the sunset hour angle for the tilted surface for the mean day of the month, which is given by:

$$\omega'_s = \min \left\{ \cos^{-1}(-\tan \varphi \tan \delta), \cos^{-1}(-\tan(\varphi - \beta) \tan \delta) \right\} \quad (10)$$

where “min” means the smaller of the two items in the brackets.

\bar{H}_T is monthly average daily total radiation on a tilted surface, R_b is monthly mean beam radiation tilt factor, \bar{H} is monthly average daily total radiation, \bar{H}_d is monthly average daily diffuse radiation, R is monthly total radiation tilt factor, ρ_G is albedo factor, ω'_s is sunset hour angle on a tilted surface by degree.

Calculating the energy required to heat the water in Dar Ghadames Hotel. These equations were used.

$$q_{hw}(t) = \rho_w Q(t) \cdot C_{pw} \cdot [T_d - T_s] \quad (11)$$

Water source temp. (T_s), Required hot water temp. (T_d), Rate hot water demand volume (Q), the water density (ρ_w) = 1000 kg/m³ and specific heat of water (C_{pw}) = 4.18 kJ/kg °C

The f-chart method estimates the fraction of a total heating load that will be provided by incidence solar radiation energy for a standard configuration of domestic heat water system which has already shown in figure 1.

$$f = 1.029 Y - 0.065 X - 0.245 Y^2 + 0.0018 X^2 + 0.0215 Y^3 \quad (12)$$

$$X = \frac{A_c F_R U_{tot} (T_{ref} - T_a) \Delta t}{L} \quad (13)$$

$$Y = \frac{A_c F_R (\tau \alpha) \bar{H}_T N}{L} \quad (14)$$

$$F_R U_{tot} = C_1 + C_2 (T_{fi} - T_a) \quad (15)$$

$$F_R (\tau \alpha) = C_0 \quad (16)$$

$$C_0 = 80 \% = 0.8, C_1 = 2.5 \text{ w/m}^2 \text{ k}, C_2 = 5.10^{-3} \text{ w/m}^2 \text{ k}$$

Where: A_c collector area (m²), f is the solar load fraction: fraction of monthly load carried by solar system, F_R is the collector heat-removal factor, L is total monthly water-heating load (J/month), T_a is monthly average ambient temperature (°C), T_r is reference temperature with a value of 60°C, U_c is collector heat-loss coefficient (W/m²·°C). Δt is number of seconds per month (s/month), $\tau \alpha$ is monthly averaged collector transmittance-absorptance product.

Note That: All equations used in this paper are based on the equations in the book of Solar Engineering of Thermal Processes, Fourth Edition, John A. Duffie and William A. Beckman [6].

Results and discussion

Ghadames is located in the far west of Libya at a longitude of 9.5° East and a latitude of 30° North, near the borders with both Tunisia and Algeria. It is known as the "Pearl of the Desert" as it is one of Libya's oldest cities, characterized by its unique architectural style. The construction of its houses is closely connected to its maze-like alleys and streets, making it appear to visitors as if it were a series of pathways and corridors. The city has a population of approximately 25,000 people. Ghadames Old City is a deeply historical site and has been classified by Enesco as a World Heritage Site.

Situated in a desert region with high solar radiation and a dry climate, where the sky is clear most days of the year, Ghadames is an ideal location for investments in solar energy projects. Such initiatives can provide electricity and water heating, contributing to sustainable development and creating new job opportunities in the region.

Dar Ghadames Hotel is one of the city's tourist landmarks, welcoming visitors throughout the year. Construction of the hotel began in 1996 by the Tunisian company Atraf and was completed in 2005. It is rated as a 4-star hotel and is owned by the Libyan Automobile and Tourism Club, a private institution established in 1969. The hotel is currently leased to Wanzrik Tourism Services Company.

The total area of the hotel site is 13 hectares, with a covered area of 6000 square meters as in the figure 4. The hotel has 68 rooms, including 32 double rooms, 32 single rooms, and 4 suites. Additionally, there is a dining hall with a capacity of 120 people, as well as a central boiler room containing 3 boilers with a capacity of 5,000 liters each. Two boilers are used for daily operations, while the third serves as a backup.

The hotel is supplied with water from the public network and fresh wells, and it has two main water tanks with a capacity of 50,000 liters.

The hotel's peak season is from early October to late April when the weather is cool to moderate. During this period the hotel accommodates about 100 guests. While the number of customers decreases during the summer due to the high temperatures and the decrease in tourist demand to less than half.

The project to install a solar water heating system at Dar Ghadames Hotel represents a step toward achieving a broader vision of adopting renewable energy sources in Libya's tourism sector. It provides an opportunity to reduce reliance on oil and gas, preserve the environment, and create new job opportunities in the region.



Figure 4. Dar Ghadames Hotel Area.

The declination and sunset hour angles can be found from the correlations 1 & 2 and the results illustrated in the table 2, while the number of daylight hours was determined by correlation 3. The site was characterized by a long number of daylight hours which makes the environment very suitable for investment.

Table 2. Estimation of the Solar Declination & sunset angles .

| months | Day of year | δ | ω_s | Ns (hours) |
|----------|-------------|----------|------------|------------|
| Jan (31) | 15 | -21.26 | 77.01 | 10.27 |
| Feb (28) | 46 | -13.28 | 82.16 | 10.96 |
| Mar (31) | 74 | -2.81 | 88.37 | 11.78 |
| Apr (30) | 105 | 9.41 | 95.49 | 12.73 |
| Mai (31) | 135 | 18.79 | 101.32 | 13.51 |
| Jun (30) | 166 | 23.31 | 104.40 | 13.92 |
| Jul (31) | 196 | 21.51 | 103.15 | 13.76 |
| Aug (31) | 227 | 13.78 | 98.14 | 13.09 |
| Sep (30) | 258 | 2.21 | 91.28 | 12.17 |
| Oct (31) | 288 | -9.59 | 84.39 | 11.25 |
| Nov (30) | 319 | -19.14 | 78.43 | 10.46 |
| Dec (31) | 349 | -23.33 | 75.57 | 10.08 |

The results obtained from the table 2 are positive, with daylight hours ranging between 10 and 14 hours. It is noticeable that the deviation between June and December daylight hours is just 4 hours. This is a good for encourage people to utilize the solar energy at this site, particularly. It shows higher sun hours in June, July and August, while lower sunshine hours were in December and January. Figure 5 shows a graphic representation of these values obtained. It represent the appropriate and natural of the radiation amounts during the months of the year within the city of Ghadames.

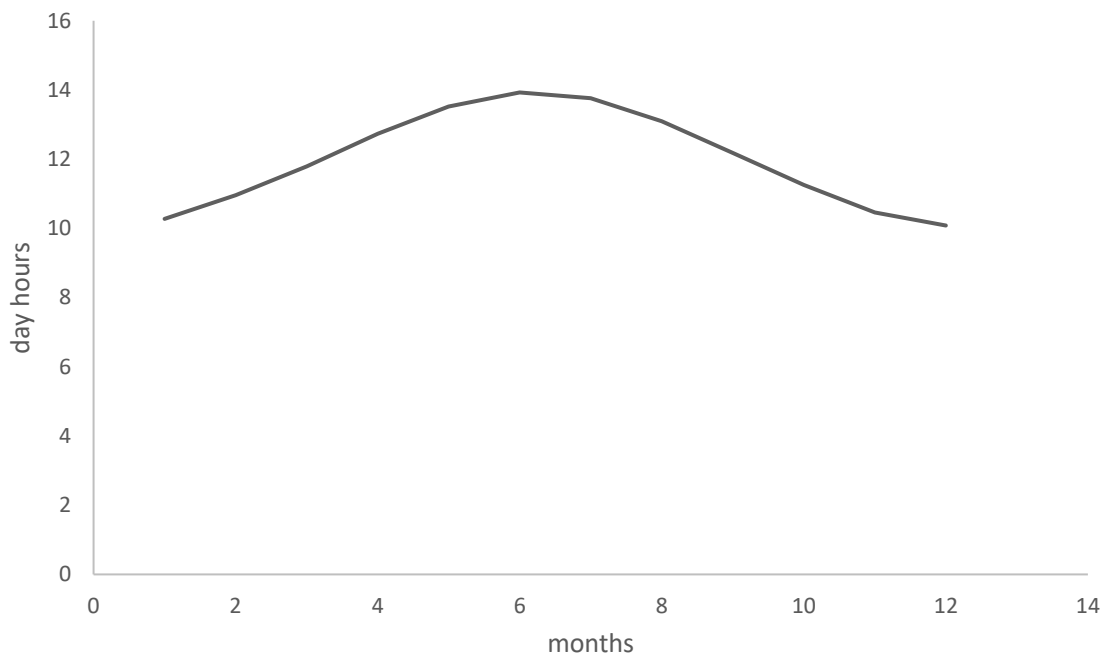


Figure 5. Number of daylight hours (N_s) for each month.

Using correlation 4 , the average monthly extra-terrestrial radiation energy (\bar{H}_o) for the city of Ghadames was estimated and presented in Table 3. The relationship between mean of the months and average monthly extra-terrestrial radiation is shown in figure 6. It is oblivious that the peaks of solar radiation were at June to August. The lowest values were around December and January. The solar constant (G_{sc}) was chosen to be 1367 w/m^2 [6].

Table 3. The Average monthly extra-terrestrial radiation for Ghadames city.

| months | Day of year | δ | ω_s | $H_o \text{ MJ/m}^2$ |
|----------|-------------|----------|------------|----------------------|
| Jan (31) | 15 | -21.26 | 77.01 | 21.06 |
| Feb (28) | 46 | -13.28 | 82.16 | 25.79 |
| Mar (31) | 74 | 2.81 | 88.37 | 31.39 |
| Apr (30) | 105 | 9.41 | 95.49 | 36.82 |
| Mai (31) | 135 | 18.79 | 101.32 | 40.02 |
| Jon (30) | 166 | 23.31 | 104.40 | 41.18 |
| Jul (31) | 196 | 21.51 | 103.15 | 40.57 |
| Aug (31) | 227 | 13.78 | 98.14 | 38.06 |
| Sep (30) | 258 | 2.21 | 91.28 | 33.40 |
| Oct (31) | 288 | -9.59 | 84.39 | 27.56 |
| Nov (30) | 319 | -19.14 | 78.43 | 22.21 |
| Dec (31) | 349 | -23.33 | 75.57 | 19.75 |

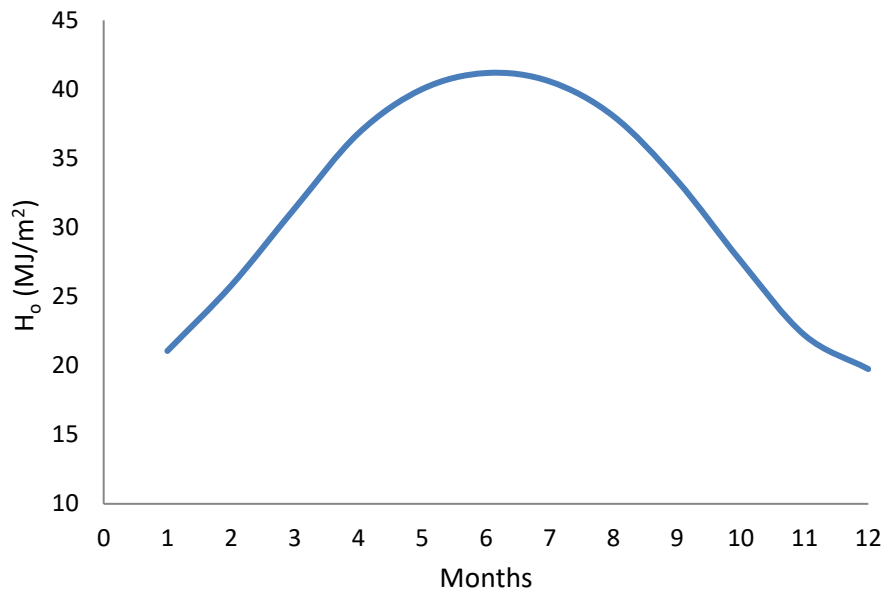


Figure 6. The Average monthly extra-terrestrial radiation (H_0) for Ghadames city.

The Clarity Indexes for Ghadames Latitude have been obtained for each month and presented in Table 4. As can be seen, the index values show good values indicating possibility of investment solar energy. The index values were around 0.6 which shows the consistency of solar energy during the year. In order to have obvious visualization, the Clarity Indexes vs. months of the year have been shown in figure 7.

Table 4. Clearance index for Ghadames city latitude.

| Months | Jan | Feb | Mar | Apr | May | Jun | Jul | Aug | Sep | Oct | Nov | Dec |
|----------------------------|------|------|------|------|------|------|------|------|------|------|------|------|
| $K_t (\varphi = 30^\circ)$ | 0.56 | 0.60 | 0.61 | 0.63 | 0.66 | 0.68 | 0.67 | 0.66 | 0.66 | 0.65 | 0.59 | 0.56 |

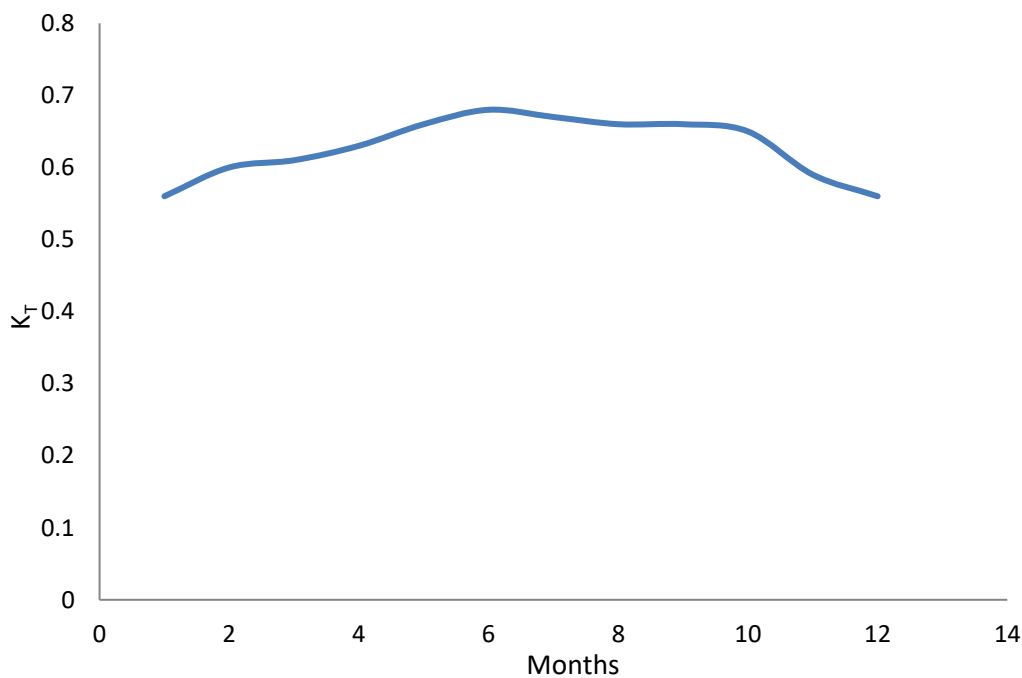


Figure 7. The average monthly clearance index (K_T) for Ghadames city latitude.

By using correlation 5, the estimation of the average monthly solar terrestrial-radiation on horizontal surface (\bar{H}_H) has been found out and presented in table 5. It obvious lowest values were during winter time (December to February) and highest vales were at summers time (June to August). It can be noted that the average monthly solar radiation within winter time has a good values with about 11 MJ/m². This indicates that the consummation energy will not be a big different between summer and winter. the relationship between average monthly solar radiation on horizontal surface and months of the year has been sketch and illustrated in figure 8.

Table 5. The average monthly solar terrestrial-radiation on horizontal surface in Ghadames city.

| Months | n | H ₀ MJ/m ² | K _T | H _H MJ/m ² |
|--------|-----|----------------------------------|----------------|----------------------------------|
| Jan | 15 | 21.06 | 0.56 | 11.80 |
| Feb | 46 | 25.79 | 0.6 | 15.48 |
| Mar | 74 | 31.39 | 0.61 | 19.15 |
| Apr | 105 | 36.82 | 0.63 | 23.20 |
| May | 135 | 40.02 | 0.66 | 26.41 |
| Jun | 166 | 41.18 | 0.68 | 28.01 |
| Jul | 196 | 40.57 | 0.67 | 27.19 |
| Aug | 227 | 38.06 | 0.66 | 25.12 |
| Sep | 258 | 33.40 | 0.66 | 22.05 |
| Oct | 288 | 27.56 | 0.65 | 17.92 |
| Nov | 319 | 22.21 | 0.59 | 13.10 |
| Dec | 349 | 19.75 | 0.56 | 11.06 |

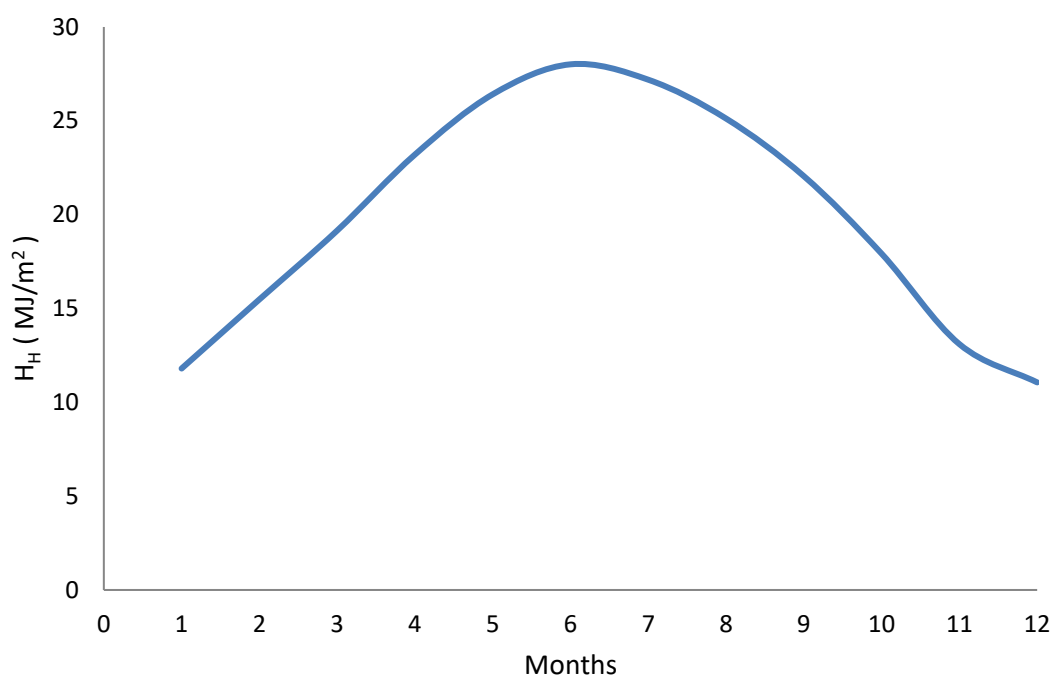


Figure 8. monthly average solar terrestrial-radiation on horizontal surface.

The optimal solar tilt angle for a collector plays an important role for the efficiency of solar energy systems. The solar flat collector surface tilted at different angles: 20°, 30°, 40°, and 60° were studied by employing correlation 6. The average monthly solar radiation at each of angle was calculated. The results were then analyzed to determine the optimal tilt angle for ensure the optimal load is obtained. The effect of collector panel inclination at each angle was presented in tables 6 to 9. Figures 9 to 11 show monthly average solar radiation at different tilted angles for each month. As can be seen from the figures, the winter shows less solar radiation energy than summer but the division between them was not large which is preferred to solar energy people.

Table 6. The monthly average solar radiation at $\beta=20^\circ$.

| Months | n | H_H [MJ/m ²] | R_b | H_d/H | R | H_T [MJ/m ²] |
|--------|-----|----------------------------|-------|---------|------|----------------------------|
| Jan | 15 | 11.79 | 2.67 | 0.48 | 1.85 | 21.85 |
| Feb | 46 | 15.47 | 2.31 | 0.41 | 1.76 | 27.34 |
| Mar | 74 | 19.15 | 1.92 | 0.39 | 1.55 | 29.83 |
| Apr | 105 | 23.20 | 1.62 | 0.35 | 1.39 | 32.38 |
| May | 135 | 26.41 | 1.46 | 0.30 | 1.31 | 34.75 |
| Jun | 166 | 28.00 | 1.39 | 0.28 | 1.28 | 35.98 |
| Jul | 196 | 27.18 | 1.42 | 0.29 | 1.29 | 35.19 |
| Aug | 227 | 25.12 | 1.55 | 0.30 | 1.38 | 34.74 |
| Sep | 258 | 22.04 | 1.83 | 0.30 | 1.57 | 34.71 |
| Oct | 288 | 17.91 | 2.22 | 0.32 | 1.82 | 32.68 |
| Nov | 319 | 13.10 | 2.60 | 0.42 | 1.90 | 24.99 |
| Dec | 349 | 11.06 | 2.82 | 0.48 | 1.92 | 21.29 |

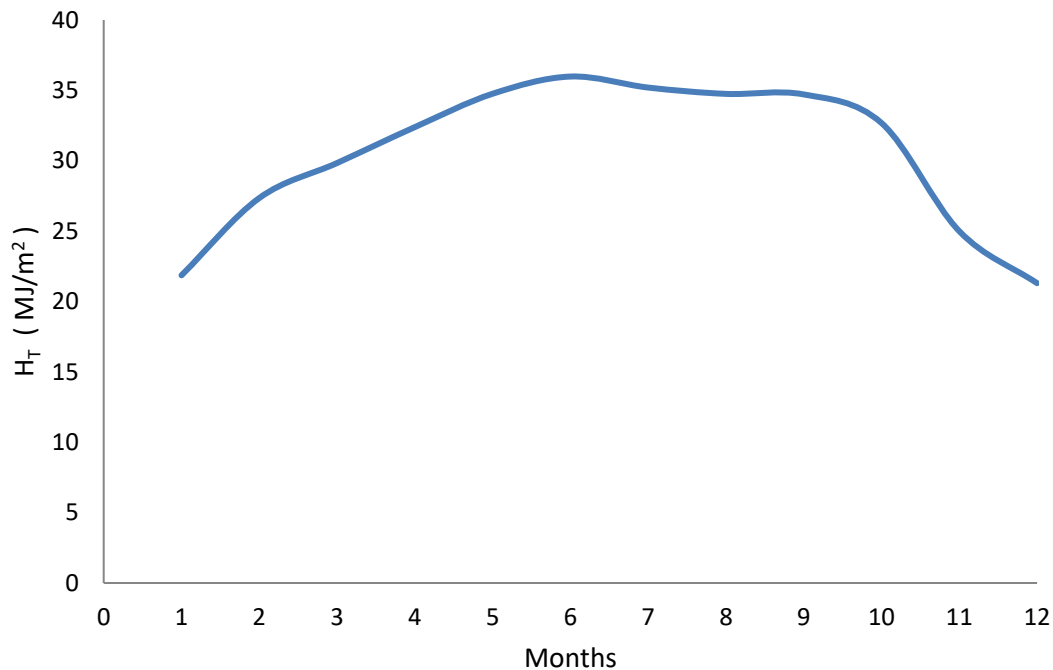


Figure 9. The monthly average solar radiation (H_T) at $\beta=20^\circ$.

Table 7. The monthly average solar radiation at $\beta = 30^\circ$.

| Months | n | H_H [MJ/m ²] | R_b | H_d/H | R | H_T [MJ/m ²] |
|--------|-----|----------------------------|-------|---------|------|----------------------------|
| Jan | 15 | 11.79 | 2.70 | 0.48 | 1.85 | 21.89 |
| Feb | 46 | 15.47 | 2.33 | 0.41 | 1.77 | 27.43 |
| Mar | 74 | 19.15 | 1.94 | 0.39 | 1.56 | 29.91 |
| Apr | 105 | 23.20 | 1.63 | 0.35 | 1.40 | 32.49 |
| May | 135 | 26.41 | 1.47 | 0.30 | 1.32 | 34.92 |
| Jun | 166 | 28.00 | 1.41 | 0.28 | 1.29 | 36.20 |
| Jul | 196 | 27.18 | 1.43 | 0.29 | 1.30 | 35.39 |
| Aug | 227 | 25.12 | 1.57 | 0.30 | 1.38 | 34.91 |
| Sep | 258 | 22.04 | 1.85 | 0.30 | 1.58 | 34.88 |
| Oct | 288 | 17.91 | 2.24 | 0.32 | 1.83 | 32.85 |
| Nov | 319 | 13.10 | 2.62 | 0.42 | 1.91 | 25.06 |
| Dec | 349 | 11.06 | 2.84 | 0.48 | 1.92 | 21.33 |

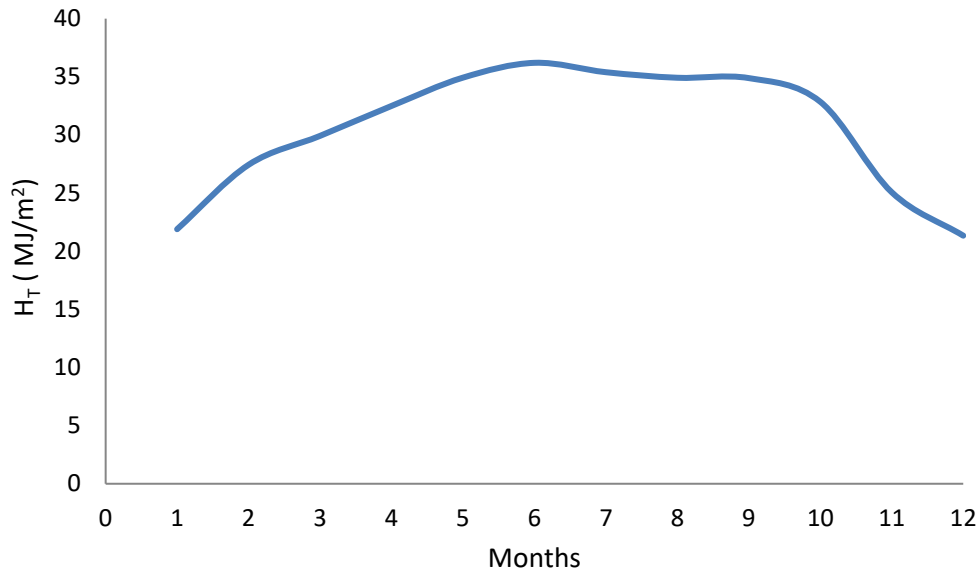


Figure 10. The monthly average solar radiation (H_T) at $\beta=30^\circ$.

Table 8. The monthly average solar radiation at $\beta=40^\circ$.

| Months | n | H_H [MJ/m ²] | R_b | H_a/H | R | H_T [MJ/m ²] |
|--------|-----|----------------------------|-------|---------|------|-----------------------------|
| Jan | 15 | 11.79 | 2.67 | 0.48 | 1.82 | 21.57 |
| Feb | 46 | 15.47 | 2.31 | 0.41 | 1.74 | 27.07 |
| Mar | 74 | 19.15 | 1.92 | 0.39 | 1.54 | 29.52 |
| Apr | 105 | 23.20 | 1.62 | 0.35 | 1.38 | 32.08 |
| May | 135 | 26.41 | 1.46 | 0.30 | 1.30 | 34.52 |
| Jun | 166 | 28.00 | 1.39 | 0.28 | 1.27 | 35.80 |
| Jul | 196 | 27.18 | 1.42 | 0.29 | 1.28 | 34.99 |
| Aug | 227 | 25.12 | 1.55 | 0.30 | 1.37 | 34.52 |
| Sep | 258 | 22.04 | 1.83 | 0.30 | 1.56 | 34.51 |
| Oct | 288 | 17.91 | 2.22 | 0.32 | 1.81 | 32.49 |
| Nov | 319 | 13.10 | 2.60 | 0.42 | 1.88 | 24.73 |
| Dec | 349 | 11.06 | 2.82 | 0.48 | 1.90 | 21.02 |

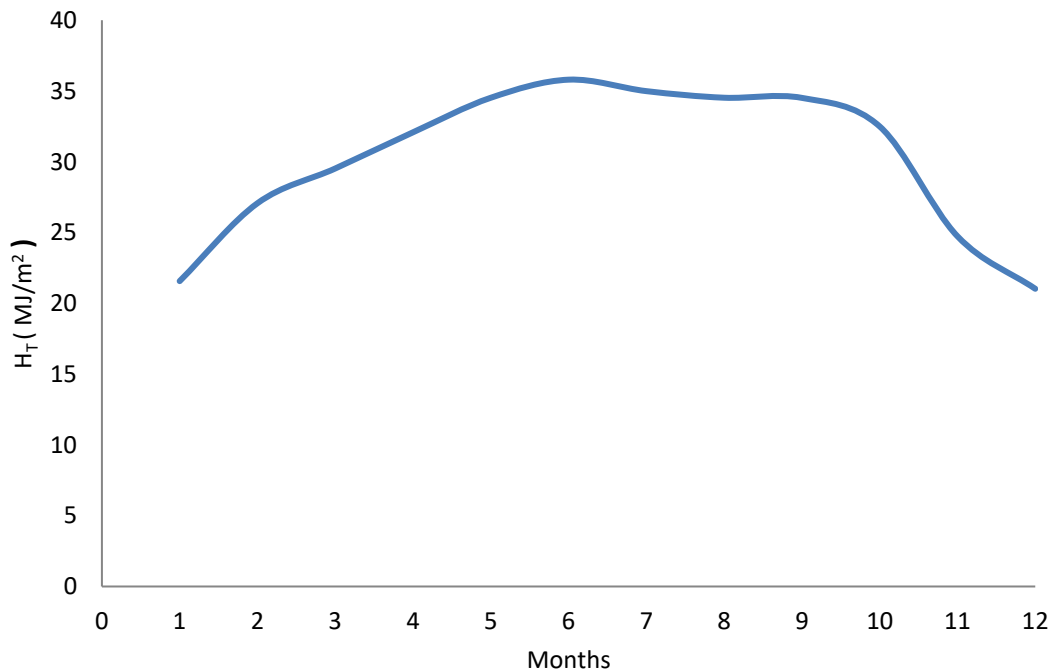


Figure 11. The monthly average solar radiation (H_T) at $\beta=40^\circ$.

Table 9: The monthly average solar radiation at $\beta=60^\circ$.

| Months | n | H_H [MJ/m ²] | R_b | H_d/H | R | H_T [MJ/m ²] |
|--------|-----|----------------------------|-------|---------|------|----------------------------|
| Jan | 15 | 11.79 | 2.45 | 0.34 | 1.91 | 22.59 |
| Feb | 46 | 15.47 | 2.11 | 0.33 | 1.70 | 26.33 |
| Mar | 74 | 19.15 | 1.76 | 0.34 | 1.45 | 27.95 |
| Apr | 105 | 23.20 | 1.48 | 0.35 | 1.27 | 29.62 |
| May | 135 | 26.41 | 1.33 | 0.34 | 1.18 | 31.24 |
| Jun | 166 | 28.00 | 1.28 | 0.34 | 1.14 | 32.19 |
| Jul | 196 | 27.18 | 1.31 | 0.34 | 1.16 | 31.75 |
| Aug | 227 | 25.12 | 1.45 | 0.34 | 1.26 | 31.76 |
| Sep | 258 | 22.04 | 1.72 | 0.32 | 1.45 | 32.10 |
| Oct | 288 | 17.91 | 2.09 | 0.31 | 1.71 | 30.75 |
| Nov | 319 | 13.10 | 2.43 | 0.33 | 1.92 | 25.21 |
| Dec | 349 | 11.06 | 2.61 | 0.34 | 2.02 | 22.41 |

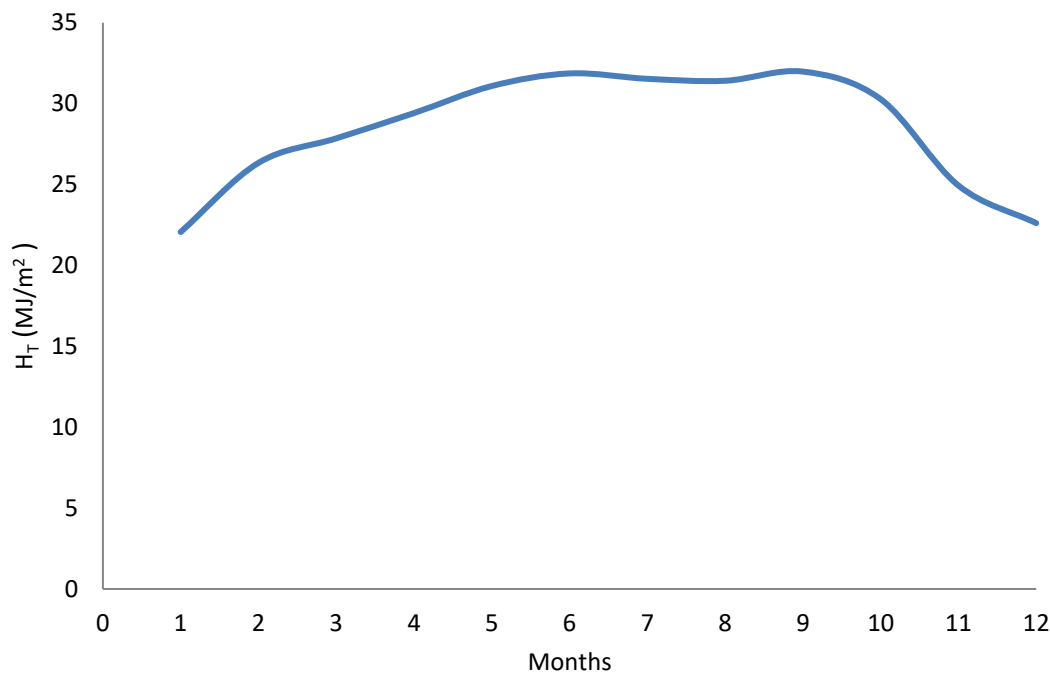


Figure 12. The monthly average solar radiation at $\beta=60^\circ$.

Table 10 summarize the monthly average solar radiation for different tilt angles. By comparing the results throughout the angles, the surface with inclination of 30° shows the maximum energy value in June (36.2 MJ/m^2) and maximum energy value in December (21.34 MJ/m^2). It is noticeable the inclination at this angle is close the city's latitude.

Figure 13 shows inclination angels of the surface as a function of mean of the months. As can be seen from the figure, that the amount of solar energy falls onto a surface with inclination angles $\beta = 20^\circ, 30^\circ$ and 40° had not significant different. This indicates that the location has a good solar energy availability year-round. Since the highest amount of solar energy is available when the surface was at tilted angle of 30° , in summer and winter, it was considered the optimal tilt angle for the collector surface at this location. These results suggest that the location is rich in solar energy making it very interesting for investment in solar energy fields.

Table 10 The monthly average solar radiation (H_T) for different tilt angles of the collector.

| H_T (MJ/m ²) | | | | |
|----------------------------|----------------|----------------|----------------|----------------|
| Months | ($\beta=20$) | ($\beta=30$) | ($\beta=40$) | ($\beta=60$) |
| Jan | 21.86 | 21.89 | 21.57 | 22.59 |
| Feb | 27.35 | 27.43 | 27.07 | 26.33 |
| Mar | 29.84 | 29.92 | 29.53 | 27.96 |
| Apr | 32.39 | 32.49 | 32.08 | 29.62 |
| May | 34.76 | 34.93 | 34.52 | 31.25 |
| Jun | 35.98 | 36.20 | 35.80 | 32.19 |
| Jul | 35.20 | 35.39 | 34.99 | 31.75 |
| Aug | 34.75 | 34.92 | 34.52 | 31.77 |
| Sep | 34.71 | 34.89 | 34.51 | 32.11 |
| Oct | 32.68 | 32.85 | 32.50 | 30.75 |
| Nov | 24.99 | 25.07 | 24.74 | 25.21 |
| Dec | 21.30 | 21.34 | 21.03 | 22.41 |

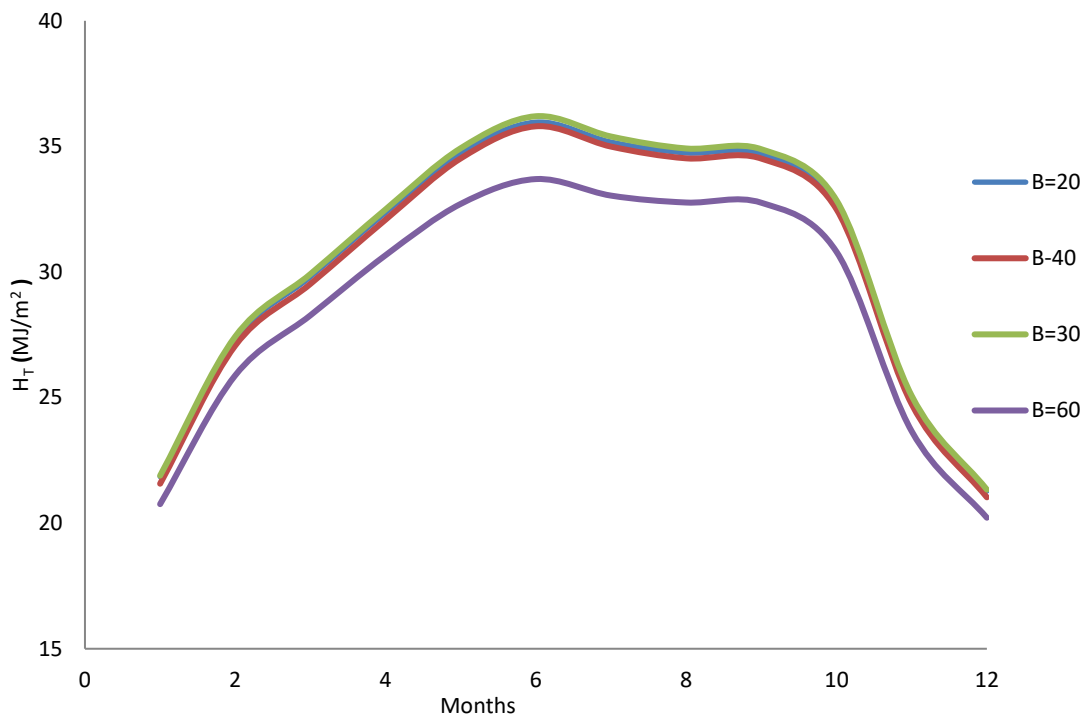


Figure 13. Inclination angles of the surface versus of mean of the months at different tilted angles $\beta=20, 30, 40$ and 60° .

The loads required to meet the demand of the hot water is determined by providing the desired water temperature. In this study, the required water temperature was considered to be 60°C . The loads related to the distribution network within the hotel depend on the number of guests in the hotel and the rate of hot water consumption. The maximum capacity of the hotel is 110 people according to the company which has been managing the hotel for about ten years, however the number of guests does not reach the maximum ranging between 70-100 in peak months and less than half in the summer. According to what was reached after field visits to a number of hotels in the city of Tripoli, the Tourism Development and Projects Authority affiliated with the Ministry of Tourism, and the General Administration of the Water and Sanitation Company affiliated with the Ministry of Water Resources, the average individual consumption of hot water is about 60 liters per day, accordingly, the demand loads for hot water can be calculated by knowing the following variables:

If the water source temperature (T_s), the required hot water temperature (T_d), and the rate of volume demand for hot water (Q). For 100 Guests the demand rate Q will be:

$Q = 100 \times 60 \text{ liters/day} = 6000 \text{ liters/day} = 6 \text{ m}^3/\text{day}$. (In the peak months). $Q = 45 \times 60 \text{ liters/day} = 2700 \text{ liters/day} = 2.7 \text{ m}^3/\text{day}$. (In the summer months). The density of water can be taken as 1000 kg/m^3 , and the specific heat, as $4.18 \text{ kJ/kg } ^\circ\text{C}$. The energy required to heat the water has been estimated by using equation 11. Table 11 summarize Monthly Water Heating Energy Demands.

Table 11. Average monthly water Heating Energy Demands for each month.

| Months | Days/Month | Q (m ³ /day | Demand (m3/month) | qw (GJ/month) |
|--------|------------|-------------------------|-------------------|---------------|
| Jan | 31 | 6 | 186 | 38.874 |
| Feb | 28 | 6 | 168 | 34.40976 |
| Mar | 31 | 6 | 186 | 34.9866 |
| Apr | 30 | 6 | 180 | 28.5912 |
| May | 31 | 2.7 | 83.7 | 13.99464 |
| Jun | 30 | 2.7 | 81 | 12.52746 |
| Jul | 31 | 2.7 | 83.7 | 12.24531 |
| Aug | 31 | 2.7 | 83.7 | 11.545578 |
| Sep | 30 | 2.7 | 81 | 11.17314 |
| Oct | 31 | 6 | 186 | 28.76676 |
| Nov | 30 | 6 | 180 | 32.3532 |
| Dec | 31 | 6 | 186 | 37.31904 |

The F-Chart method is a simple and effective graphical technique used in the design and analysis of solar water heating system and as well as for estimating the performance of the system. It was developed in the 1970 by Dr. Duffy and Dr. Beckman [6]. The F-Chart method is based on sketching curves that represent the expected performance of a solar water heating system based on several factors such as the amount of solar radiation obtained from the solar collector, the amount of heat required for different applications, the specifications of the solar collector and its absorption, insulation and storage system characteristics. In this manner, the specific annual solar load fraction (the ratio of annual solar load fraction to area) has been calculated using correlation 12 and illustrated in table 12.

Table 12. Annual solar load fraction (f).

| Months | Days (Month) | Q m3/day | Demand (m3/month) | qw (J) | f |
|--------|--------------|----------|-------------------|----------------|--------|
| Jan | 31 | 6 | 186 | 1254000000 | 0.3858 |
| Feb | 28 | 6 | 168 | 1228920000 | 0.4385 |
| Mar | 31 | 6 | 186 | 1128600000 | 0.5577 |
| Apr | 30 | 6 | 180 | 953040000 | 0.6715 |
| May | 31 | 2.7 | 83.7 | 451440000 | 1.1939 |
| Jun | 30 | 2.7 | 81 | 417582000 | 1.2448 |
| Jul | 31 | 2.7 | 83.7 | 395010000 | 1.281 |
| Aug | 31 | 2.7 | 83.7 | 372438000 | 1.307 |
| Sep | 30 | 2.7 | 81 | 372438000 | 1.285 |
| Oct | 31 | 6 | 186 | 927960000 | 0.710 |
| Nov | 30 | 6 | 180 | 1078440000 | 0.481 |
| ec | 31 | 6 | 186 | 1203840000 | 0.386 |
| | | | | 9783708000 (J) | |
| | | | | 9.783708 (GJ) | |

According to the equations and based on the characteristics of the collector from the approved tables, the results were obtained. figure 14 show the annual solar load fraction at different surface area. It was noticed that the most suitable area for this specific load was 20 m². This area is sufficient to cover 97% of the load with the remaining load being coverable, if necessary through the main grid.

The optimal annual system was designed to supply Dar Ghadames Hotel with hot water at a temperature of 60 degrees throughout the year, including the peak period when the load is 100 guests, as well as covering the demand during the summer period when the load is less than half. The design was to install the solar collector on top of the building near the boiler room and tanks.

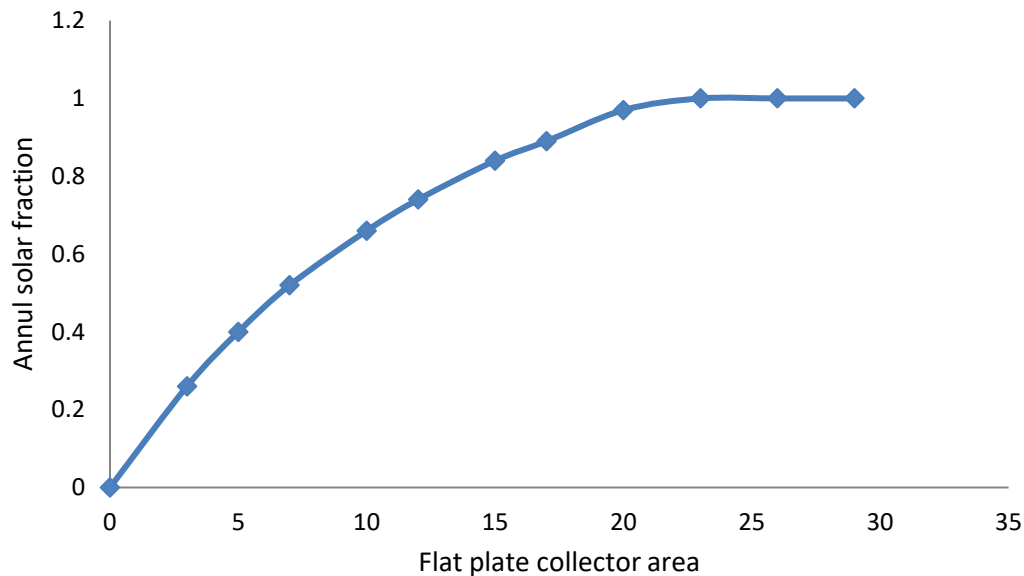


Figure 14. The annual load fraction vs. collector area (f-chart curve).

The conclusion

In this research conducted to design a solar water heating system for Dar Ghadames Hotel, the necessary site data obtained from the National Center of Meteorology were used along with mathematical equations from the book Solar Engineering for Thermal Processes, by John A. Duffie and William A. Beckman. A flat plate solar collector was chosen for this study with the following characteristics $F_R(\tau\alpha) = C_0 = 80\% = 0.8$, $C_1 = 2.5 \text{ W/m}^2 \text{ k}$, $C_2 = 5.10^{-3} \text{ W/m}^2 \text{ k}$.

It is considered the most suitable in terms of meeting the required temperatures and cost effectiveness. Solar radiation data were collected and the monthly average of extra-atmospheric and intra-atmospheric solar radiation on a horizontal surface was calculated. The monthly average of solar radiation inside the atmosphere was also calculated on the inclined surfaces at different angles (20, 30, 40, 50, 60) to determine the optimal angle of inclination. It was found that the best angle of inclination is 30 degrees towards the south, through which the maximum amount of solar energy needed to heat water, can be obtained in the appropriate amount to cover the load in the hotel and at the required temperature of 60 degrees Celsius. The f-chart method was used to calculate and optimize the area of the suitable solar collector area for the system in this location, which was 20 square meters. This is an appropriate area to cover the load of the hotel required during a year. Any increase in the number of solar panels means an increase in costs. The results also showed that the site has a good enough of solar energy. It was found that the maximum intensity of solar radiation reached (36.20 MJ/m^2) in June and the lowest value reached (21.33 MJ/m^2) in December. This amount of energy is sufficient to meet the site's needs, which amount to (38.874 GJ/month).

Compliance with ethical standards

Disclosure of conflict of interest

The authors declare that they have no conflict of interest.

References

1. International Energy Agency. 2022 report.
2. IRENA. 2022 report.
3. Cooper, P. I. (1969). The absorption of solar radiation in solar stills. *Solar Energy*, 12(3), 333–346.
4. <https://www.astrojem.net/translation-of-the-earth-around-the-sun-at-106-000-km-hour>.
5. John A. Duffie and William A. Beckman, *Solar Engineering of Thermal Processes* 1977 (Wiley).
6. Duffie, J. A., & Beckman, W. A. *Solar Engineering of Thermal Processes*, Fourth Edition. John Wiley & Sons, Inc, 2013.
7. G. E. A. Muftah, Mohamed Husayn Alzaaluk, Optimize tilted angle of PV panel subjected to Tripoli microclimate condition, *Albahit Journal of Applied science* 4 (2025) 1.

Disclaimer/Publisher's Note: The statements, opinions, and data contained in all publications are solely those of the individual author(s) and contributor(s) and not of LJCAS and/or the editor(s). LJCAS and/or the editor(s) disclaim responsibility for any injury to people or property resulting from any ideas, methods, instructions, or products referred to in the content.